3-2016

Experimental study on the thermal characteristics of micro channel separate heat pipe respect to different filling ratio

Li Ling
Hunan University

Quan Zhang
Hunan University, quanzhang@hnu.edu.cn

Yuebin Yu
University of Nebraska–Lincoln, yyu8@unl.edu

Shuguang Liao
Changsha Maxxom High-tech Co. Ltd., Changsha, Hunan

Zhengyong Sha
Xiangjiang Technology Co. Ltd, Yangzhong, Jiangsu

Published in *Applied Thermal Engineering* 102 (2016), pp. 375–382. doi 10.1016/j.applthermaleng.2016.03.016

Submitted December 21, 2015; accepted March 5, 2016; published online March 19, 2016.

Experimental study on the thermal characteristics of micro channel separate heat pipe respect to different filling ratio

Li Ling,[1] Quan Zhang,[1] Yuebin Yu,[2] Shuguang Liao,[3] and Zhengyong Sha [4]

1 College of Civil Engineering, Hunan University, Changsha, Hunan 410082, China
2 Durham School of Architectural Engineering and Construction College of Engineering, University of Nebraska–Lincoln, Omaha, NE 68182, USA
3 Changsha Maxxom High-tech Co. Ltd., Changsha, Hunan 410015, China
4 Xiangjiang Technology Co. Ltd, Yangzhong, Jiangsu 21200, China

Corresponding authors
Q. Zhang, College of Civil Engineering, Hunan University, No. 2 Lushan South Road, Yuelu District, Changsha 410082, China; tel +86 731 8882 1254; fax +86 731 8882 1005 ; email quanzhang@hnu.edu.cn
Y. Yu, Durham School of Architectural Engineering and Construction College of Engineering, University of Nebraska–Lincoln, Omaha, NE, 68182, USA; tel +1 402 554 2082; email yuebin.yu@unl.edu

Abstract
A micro channel separate heat pipe (MCSHP) that can use natural cold energy was developed to reduce the cooling energy consumptions of telecommunications stations (TSs). Experimental investigations of exploring the optimal refrigerant filling ratio of MCSHP under different outdoor conditions and flow rates were presented. R22 was used as the working fluid. Various refrigerant filling ratios were tested in an enthalpy difference laboratory (EDL) in order to determine the optimal thermal performance for the exterior space temperature range from 8 °C to 23 °C and the air volume flow rate range from 1712 m^3/h to 2980 m^3/h. In addition, transient and steady-state performance under the optimal refrigerant filling ratio of the MCSHP was studied. As a result of experiments, the optimal refrigerant filling ratio was found in the range from 88% to 101% for different exterior conditions and airflow rates. For the optimal refrigerant filling ratio, the startup time was about 1100 s and then the refrigerant pressures entered a steady state. The cooling capacity and energy efficiency ratio (EER) increased with increasing temperature difference between the indoor and the outdoor; these values were high to 7440W and 23, respectively, at temperature difference 20 °C. The results are useful for the design and operational control of the MCSHP for TSs.
Keywords: Micro channel separate heat pipe, Refrigerant filling ratio, Thermal characteristics, Transient state, Energy efficiency ratio

1. Introduction

In recent years, with the rapid development of telecommunication industry, millions of telecommunication stations (TSs) have been built. The communication network in China has grown as the largest one in the world with over 600,000 stations in 2007 [1]. Operation of such a huge network consumes about 20 billion kW h electricity annually, one third of which is accounted by TSs [2]. To ensure the proper operation of electronic equipment inside [3,4], a large amount of energy is consumed by the equipped air-conditioning systems to keep the temperature, relative humidity and cleanness of the indoor air. The electricity consumption of these air-conditioning systems is of great significance and comprises about 30–50% of the total [5]. To save the primary energy, alternative heating and cooling technologies, such as a heat pipe, that can make use of natural thermal resources, is promising. Compared to the best available thermal conductors, heat pipe's heat transfer capability can be 500 times larger. It greatly improves the heat transfer capability with a small cross-section area and over a longer distance without consuming power for refrigerant compressors.

The application of heat pipe for TSs received wide attention recently. For example, Ekstedt and Johansson [6] designed a radio base station with a loop thermosyphon, a device similar to a heat pipe, through a heating conducting wall; Weber and Wyatt [7] designed a data center utilizing heat pipe. Subsequently, Samba et al. [8] proposed a two-phase thermosyphon loop for cooling telecommunication equipment in the outdoor cabinet. Zhou et al. [9] have reported energy-saving analysis of telecommunication base station with thermosyphon heat exchangers. It was found that the annual energy savings were over 30% in cold and moderate zones. Furthermore, in order to improve the performance of a heat pipe system, Tian et al. [10] proposed a multi-stage heat pipe loop to improve the indoor thermal environment and reduce annual cooling cost by approximately 46% of data rooms. Among these studies, most heat pipe systems applied in TSs cooling system were constructed

Nomenclature

List of abbreviations

EDL	enthalpy difference laboratory
EER	energy efficiency ratio
MCSHP	micro channel separate heat pipe
RTPF	round tubes and plate fins
SHP	separate heat pipe
TSs	telecommunication stations

List of symbols

A_0	total air side surface area, m^2
FR	Refrigerant filling ratio, %
G	mass flow rate, kg s^{-1}
H	enthalpy, J kg^{-1}
h	heat transfer coefficient, W/(m^2 K)
P	pressure, Pa
P_{sys}	power of the micro channel separate heat pipe system, W
Q	cooling capacity, W
R	thermal resistance, °C/W
T	temperature, K
V	airflow rate, m^3 s^{-1}
V_e	volume of the evaporator section, m^3
V_i	refrigerant volume, m^3
V'_n	specific volume of air at nozzle, m^3 kg^{-1}
W_n	humidity ratio of air at nozzle, kg kg^{-1} (dry air)

Greek symbols

η_0	surface effectiveness

List of the subscripts

a	air, air side
c	condenser section
e	evaporator section
in	inlet
out	outlet
s	saturation
sc	subcooling
sh	superheating

with round tubes and plate fins (RTPF), while little information on separate heat pipe (SHP) with micro channel heat exchangers was reported. A micro channel separate heat pipe (MCSHP) has advantages such as better heat transfer, lower pressure drop and more compact structure compared to heat pipe with RTPF. Among the limited studies, Zhang et al. [11] experimentally investigated the heat recovery efficiency of a new-type flat microheat- pipe-array heat exchanger with different volume friction nanofluids, air volume flow rates and inlet air temperature of evaporator section; Ling et al. [12] developed a steady state model to analyzed effects of geometrical design on the overall thermal performance of MCSHP.

As a regular refrigerant cooling cycle, the thermal performance of a heat pipe system can be greatly impacted by the working fluid filling ratio. Samba et al. [8] measured the effect of the refrigerant filling ratio (defined as the ratio between the working fluid volume and the thermosyphon loop volume) varying from 2.4% to 14.8% under heat loads changing from 150 to 550 W. It obtained the lowest operating temperature at the filling ratio 9.2%. Noie [13] experimentally analyzed the effects of the input heat transfer rates, the working fluid filling ratio, and the evaporator lengths (aspect ratios) on the heat transfer performance in a two-phase, closed thermosyphon. The filling ratio in his study was defined differently as the ratio of working fluid volume to the volume of the evaporator section. It was found that the optimal filling ratio at different aspect ratio was different. For aspect ratios of 11.8, 9.8 and 7.45 the corresponding filling ratios for maximum heat transfer rate are 60%, 30% and 90%, respectively. Liu et al. [14] developed a steady state model to determine the upper and lower boundaries of filling ratio for looped two-phase SHP for an air conditioning exhaust system; however the optimal filling ratio was not indicated for the system. Armijo and Carey [15] did an analytical and experimental study on an inclined gravity-assisted heat pipe for several liquid charge ratios between 30% and 70%. It was found that the heat pipe has the lowest overall superheat and highest critical heat flux at 45% liquid charge. Chen and Chou [16] showed experimentally the effects of filling ratios and leakage on the cooling performance of flat plate heat pipes. It obtained the best performance at 25% filling ratio between the working fluid volume and the flat plate heat pipe volume.

Among these studies on the filling ratio, researchers mainly focused on the thermal performance of thermosyphon or SHP by evaluating the evaporator section surface temperature and the heat transfer rate. Very little information was revealed from the refrigerant side, such as the working fluid temperatures and pressures at the evaporator section and the condenser section inlet and outlet, superheating at evaporator section exit and subcooling at condenser section exit, which dominates the heat transfer mechanism. Secondly, these studies investigated the effect of filling ratio on the basis of different heat loads or inlet air temperature of the evaporator section, which differs greatly from the indoor environment in TSs where the indoor temperature and relative humility are required in a relatively small range. Unlike the evaporator superheating test or subcooling test of common mechanical vapor compression airconditioners, empirical values obtained from repeated tests in rated condition are generally used by SHP manufacturers to determine the filling ratio. Results from SHP manufacturers are limited to the rated conditions without considering the variation of outdoor condition and airflow rate. Meanwhile, the refrigerant mass flow rate of a MCSHP is much lower than that of a compression refrigeration system; the operating pressures, temperatures and heat transfer coefficient of evaporator section and condenser section are also different from micro channel heat exchangers applied in a mechanical compression refrigeration system [17,18]. Traditional twophase heat transfer coefficient cannot be used to predict the evaporating and condensing process of MCSHP.

This paper seeks to fill in the gap outlined above and determine the optimal refrigerant filling ratio of MCSHP under different outdoor conditions and flow rate experimentally for TSs. Firstly, we briefly introduce the MCSHP and the test facility. Then, we present the test results obtained from the experiments with various refrigerant filling ratios. The optimal filling ratio is obtained by evaluating the thermal performance with different outdoor air conditions and air volume flow rates; the cooling capacity, energy efficiency ratio (EER), refrigerant temperatures and pressures of evaporator section and condenser section inlet and outlet, superheating of evaporator section exit, and subcooling of condenser section exit are analyzed. Finally, the transient and steady-state thermal characteristics of the MCSHP were studied under the optimal refrigerant filling ratio. We conclude this paper with a brief discussion.

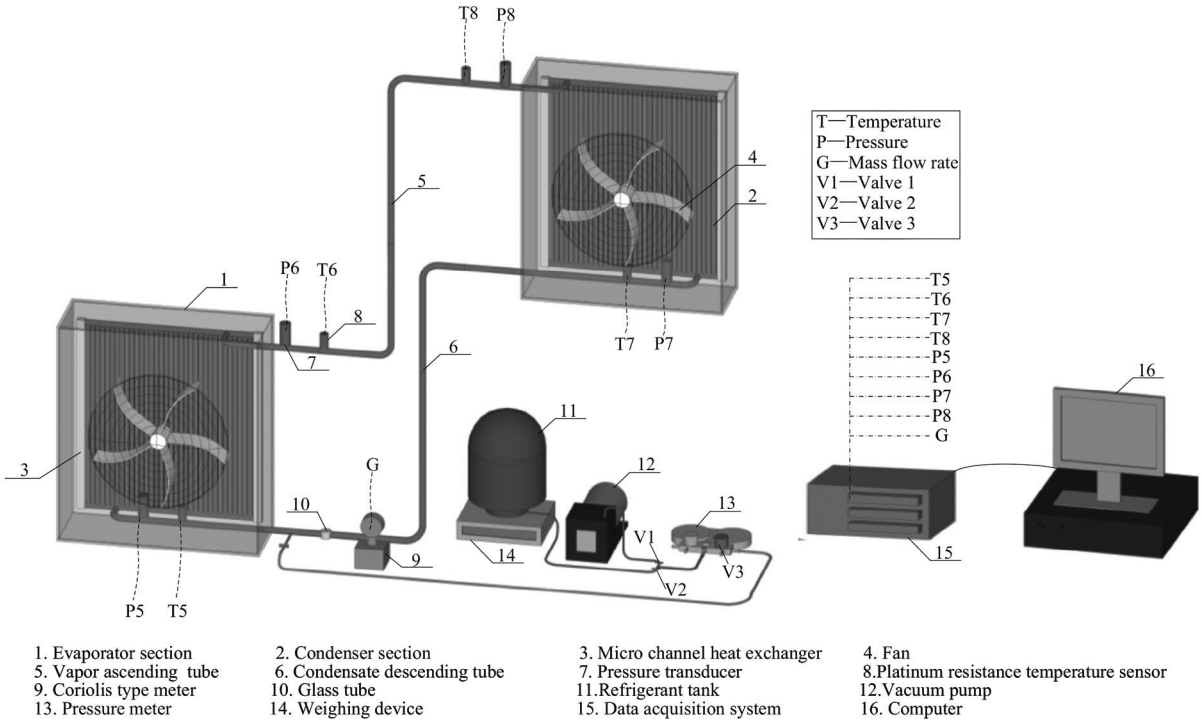

Figure 1. Micro channel separate heat pipe and testing devices.

Table 1. Geometrical parameters of the test sample.

Parameter	Value	Parameter	Value
Evaporator section core size (mm)	750 – 780 – 25	Web thickness δ_w (mm)	0.4
Condenser section core size (mm)	800 – 820 – 25	Fin pitch P_f (mm)	1.5
Number of micro-channel in one flat tube N_w	18	Fin height H_f (mm)	8
Flat tube width B_{to} (mm)	25	Fin thickness δ_f (mm)	0.1
Flat tube height H_{to} (mm)	2	Louver pitch P_l (mm)	1
Flat tube thickness δ_t (mm)	0.3	Louver length L_l (mm)	7
Fin width B_f (mm)	25	Louver angle (deg)	30

2. Experimental setup

2.1. Description of micro channel separate heat pipe

The MCSHP developed for cooling TSs is illustrated in Figure 1. It comprises a closed circuit, containing an evaporator section and a condenser section where the working fluid evaporates and condenses respectively. The condenser section is located above the evaporator section 2.0 m so that the refrigerant condensate returned to the evaporator section by gravity. The vapor ascending tube, 3.66 m long and 19 mm outer diameter, is located between the evaporator section outlet and the condenser section inlet. The condensate descending tube connecting the condenser section outlet to the evaporator section inlet is 4.37 m long with a 16 mm outer diameter. R22 is used as the working fluid because of the high figure of merit (an index to measure the working fluid effectiveness upon the physical and thermal properties) at normal temperature (5–28 °C) conditions [19]. The evaporator and the condenser of MCSHP are made of a cabinet, a micro channel heat exchanger and a fan. The fan of the evaporator section and condenser section are both axial fans (model: YDF74L6-522N-450 and YWFA6S-450S-7DIIIA01). Compared to RTPF, micro channel heat exchangers possess better heat transfer performance of capacity, lower refrigerant pressure drop, lower filling charge and more compact structure [20,21]. The micro channel structure is considers as an effective ways to improve the system energy efficiency. The refrigerant flow inside and the air flow outside the micro channel heat exchanger are oriented in cross flow. For the test sample, the section area of the micro channels is rectangular and its hydraulic diameter is approximately 1.09 mm. The interior of each flat tube contains several webs (cells), which are utilized to enhance the performance of heat transfer and make the structure more compact. Design of multi-louver fins increases the heat transfer area and improves the efficiency of heat transfer. The main geometric parameters of the test sample are summarized in Table 1.

2.2. Test facility

The thermal characteristics tests of the MCSHP were carried out in an enthalpy difference laboratory (EDL), which was mainly used to emulate the working environment for an MCSHP. The EDL is composed of interior space, exterior space and a control panel as shown in Figure 2. The interior space of the lab was used to emulate the indoor air dry-bulb and wet-bulb temperatures as the indoor conditions of TS, and the exterior space for emulating the outdoor environment. Probes at measuring location ① and ② measured and recorded the dry-bulb and wet-bulb temperatures of the air at the exit of the evaporator section and the nozzle air, respectively. The indoor and outdoor air dry-bulb and wet-bulb temperatures were measured and recorded by probes at locations ③ and

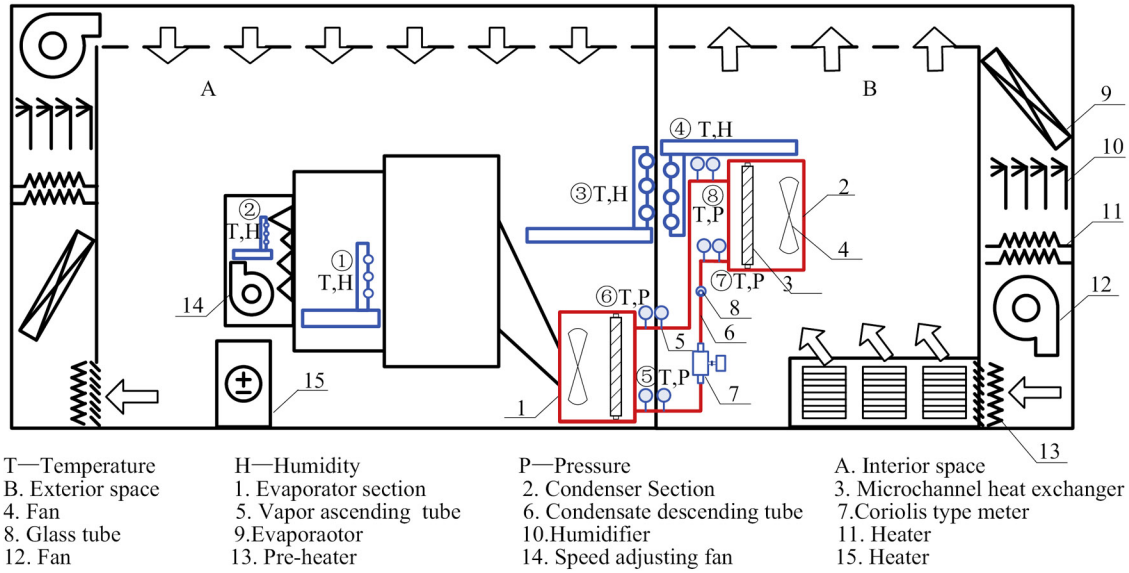

Figure 2. Schematic diagram of the enthalpy difference laboratory (EDL).

④, respectively. The air volume flow rate was adjusted by adding a pressure drop across the nozzles.In order to characterize the heat transfer mechanism of the MCSHP, measurements on the temperatures, pressures and mass flow rate of the refrigerant were necessary; these probes were installed as shown in Figure 2. The refrigerant mass flow rate was measured by using a Coriolis type meter and installed at the condensate descending tube. A glass tube was provided in the condensate descending tube near the condenser section for visualizing the flow regimes as well as the presence of fluctuations of the flow in the system. Refrigerant temperatures and pressures before and after the evaporator section and the condenser section were measured using platinum resistance temperature sensors ⑤–⑧ and pressure transducers ⑤–⑧, respectively.

During test period, the temperature of air side, air volume flow rate, current, voltage and power were recorded by EDL and the temperatures, pressures and mass flow rate parameters of refrigerant side were recorded in the data acquisition system. The major sensors and their models, errors and ranges are collected in Table 2. The cooling capacity of the evaporator section was calculated using the enthalpy difference between the inlet and outlet of evaporator section air enthalpy. Base on the uncertainty calculation method proposed by Moffat [22] and the sensors' errors in Table 2, the measurement uncertainty of evaporator section cooling capacity is 6.8%.

2.3. Test condition

In order to determine the optimal refrigerant filling ratio of MCSHP under different outdoor conditions and flow rates, and analyze the transient and steady-state thermal characteristics of MCSHP under the optimal refrigerant filling ratio, this experiment test conditions shown in Table 3 were used. The refrigerant filling charge changed from 0.8 kg to 3.8 kg. This experiment was carried out under a simulation of TS conditions, in which the interior space air dry-bulb and wet-bulb temperatures were kept at 28 °C and 19.3 °C, respectively, and the exterior space air dry-bulb temperatures were varied from 8 °C to 23°C with a constant relative humidity maintained at 45% for consistency. According to the psychrometric chart under atmospheric pressure 999.40 kPa, Condition 2 is set as the standard condition according to the standard YD/T 2770-2014 [23]. The air volume flow rate of evaporator section has two modes.

Table 3. Test conditions for MCSHP.

	Range
Refrigerant filling charge (kg)	0.8, 1.0, 1.2, 1.4, 1.6, 1.8, 2.2, 2.6, 3.0, 3.4, 3.8
The exterior space air conditions	23/15.3 (Condition 1), 18/11.4 (Condition 2),
(Dry/wet bulb temperature) (°C)	13/7.4 (Condition 3), 8/3.4 (Condition 4)
The air flow rate (m^3/h)	2980 (Mode 1), 1712 (Mode 2)

2.3.1. Refrigerant filling ratio determination test

It is necessary to determine the optimal refrigerant filling ratio of the MCSHP to achieve the best performance under different outdoor conditions and air volume flow rates. Before starting the test, a vacuum pump was utilized to remove the air in the MCSHP. As shown in Figure 1, Valves 1 and 3 were turned on and Valve 2 was turned off. After this process, Valve 1 was turned on and Valve 2 was turned off to charge working fluid through the fill charge

Table 2. Major sensors and their errors and ranges.

Types	Probes ①–④		Probes ⑤–⑧			Flow rate (m^3/h)	Current (A)	Voltage (V)
	Dry-bulb temperature (°C)	Wet-bulb temperature (°C)	Temperature (°C)	Pressure (kPa)	Mass flow rate (kg/h)			
Model	WZPK-176S		PT100	AKS32-060G2037	DMF-1-3-B	–	EP2048967B	
Errors	0.1	0.1	0.1	7.5	1	0.03	0.2	2.5
Ranges	–15 to 55	–15 to 55	–30 to 200	–100 to 240	0–300	1395–4217	0.01–40	5.0–500

line. After charging the experimental loop, Valve 3 is switched off to start the test. For different exterior conditions and different air volume flow rates, eleven different refrigerant filling charges were tested. The recorded parameters include air dry-bulb and wet bulb temperatures, refrigerant pressures, refrigerant temperatures, refrigerant mass flow rate, air volume flow rate, current, voltage, power and cooling capacity.

2.3.2. Transient state response under standard condition test

In order to reduce the effect of random errors on the accuracy of the transient state thermal response, an experiment was repeated three times with the optimal refrigerant filling ratio under standard condition to investigate the transient state thermal performance. Each time, the refrigerant was charged through the fill charge line as described in the previous section. After the working fluid was charged and the fans were switched on, the EDL and data acquisition system recorded experimental parameters.

2.3.3. Cooling capacity and EER under different conditions test

In the present study, the MCSHP were experimented comprehensively under four different conditions to investigate the effects of temperature difference between interior and exterior space. All the detailed conditions setup was listed in Table 3. The experimental procedures were presented in Section 2.3.1.

3. Results and discussion

3.1. Determination of the optimal filling ratio

Working fluid filling ratio in the MCSHP plays a significant role. If the working fluid filling ratio is low, there is a risk of drying out in the evaporator section; the upper section of the evaporator inner wall has no liquid film cover, leading to a rapid wall temperature increase and thermal performance degradation. If the working fluid filling ratio is high, it will cause excessive fluid to accumulate in the condenser section. Thereby increasing the subcooling at the condenser exit and decreasing the thermal performance [15]. An optimal filling ratio exerts a pivotal role in the MCSHP to ensure that the telecommunication equipment in TS can operate safely and efficiently.

In this process, the cooling capacity, the energy efficiency ratio (EER), the superheating of the evaporator section outlet and the subcooling of the condenser section outlet as the objective parameters were applied to evaluate the thermal characteristics of MCSHP.

The refrigerant filling ratio is defined by Equation (1):

$$\mathrm{FR} = \frac{V_i}{V_e} \times 100\% \tag{1}$$

where FR is the refrigerant filling ratio, V_i is the refrigerant volume at 20 ℃, and V_e is the volume of the evaporator section.

The cooling capacity of evaporator section was calculated using the enthalpy difference between the inlet and outlet of evaporator section air temperature [24], as follows:

$$Q = \frac{V(h_{a,in} - h_{a,out})}{V'_n\,(1 + W_n)} \tag{2}$$

where Q is the cooling capacity of the evaporator section, $h_{a,in}$ and $h_{a,out}$ are the respective air enthalpy at the evaporator section inlet and outlet, V is the volumetric flow rate, V'_n is specific volume of air at nozzle, and W_n is the humidity ratio of air at nozzle.

The EER is defined by Equation (3):

$$\mathrm{EER} = \frac{Q}{P_{sys}} \tag{3}$$

where EER is the energy efficiency ratio and P_{sys} is power of the fans.

The superheating at the evaporator section outlet was calculated to evaluate the working fluid heat transfer characteristics of evaporator section:

$$T_{sh} = T_{e,out} - T(P_s)\big|_{P_s = P_{e,out}} \tag{4}$$

where T_{sh} is the superheating at the evaporator section outlet, $T_{e,out}$ and $P_{e,out}$ are the refrigerant temperature and pressure at the evaporator section outlet, and $T(P_s)$ is the saturation temperature of refrigerant respective to the refrigerant pressure at the evaporator section outlet.

The subcooling at the condenser section outlet was obtained to evaluate the working fluid heat transfer characteristics of condenser section, as follows:

$$T_{sc} = T_{c,out} - T(Ps)\big|_{P_s = P_{c,out}} \tag{5}$$

where T_{sc} is the subcooling at the condenser section outlet, $T_{c,out}$ and $P_{c,out}$ are the refrigerant temperature and pressure at the condenser section outlet, and $T(P_s)$ is the saturation temperature of refrigerant respective to refrigerant pressure at the condenser section outlet.

3.1.1. Determination of the optimal filling ratio for different exterior conditions

Considering the actual operation, the condenser section of the MCSHP was installed outdoor. Therefore, the experiments were conducted under different refrigerant filling ratios for Conditions 1–4 to determine the optimal filling ratio. The results were collected when the system reached a steady-state for all the experiments. Figure 3 shows the cooling capacity measured in the steadystate as a function of different refrigerant filling ratios for different conditions. For a given refrigerant filling ratio, the cooling capacity of the evaporator section increased with the decrease of outdoor air temperatures because the decrease of the outdoor air temperature caused a decrease of the operating temperature of the MCSHP. Therefore, the outlet air temperatures of the evaporator section decreased (as shown in Figure 4), and led to the increased cooling capacity. For Condition 1, the maximum cooling capacity could be obtained up to 1677W for the refrigerant filling ratio from 57% to 107%. For Condition 2–3, the optimal filling ratio range was about 82–107% and the cooling capacity were 3979.70W and 5831.2 W, respectively. For Condition 4, the maximum cooling capacity was 7438W at refrigerant filling ratio 95%.

For a given air side inlet condition, with a refrigerant charge ration smaller than the optimal region, less refrigerant could reach the evaporator, thereby decreased the area of effective evaporator surface. Consequently, the superheating at the evaporator exit increased and the heat transfer rate decreased. With the increase of the refrigerant ratio, the heat transfer rate increased and the

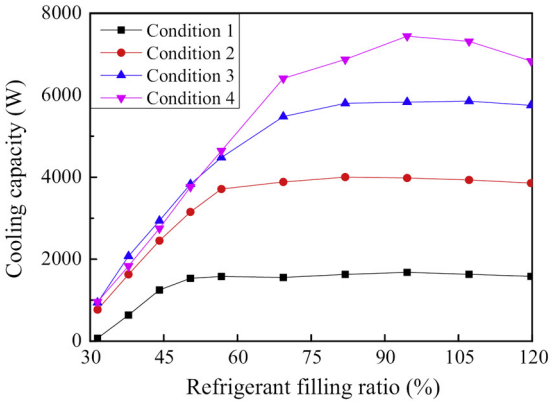

Figure 3. Cooling capacity under different refrigerant filling ratios for different conditions.

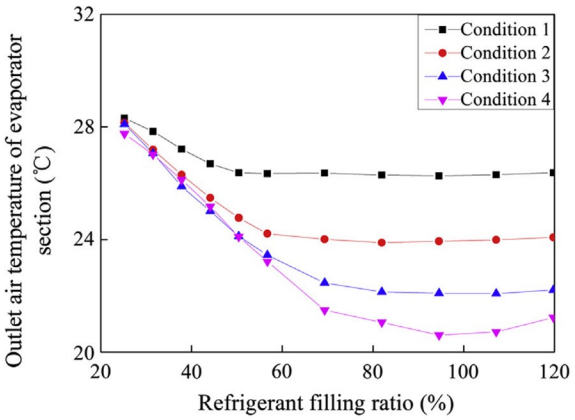

Figure 4. Outlet air temperatures of evaporator section under different refrigerant filling ratios for different conditions.

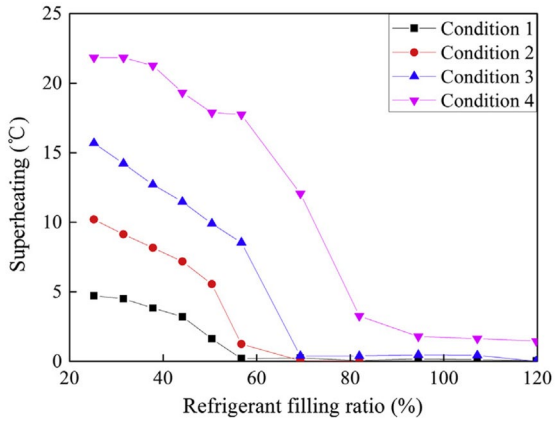

Figure 5. Superheating under different refrigerant charges for different conditions.

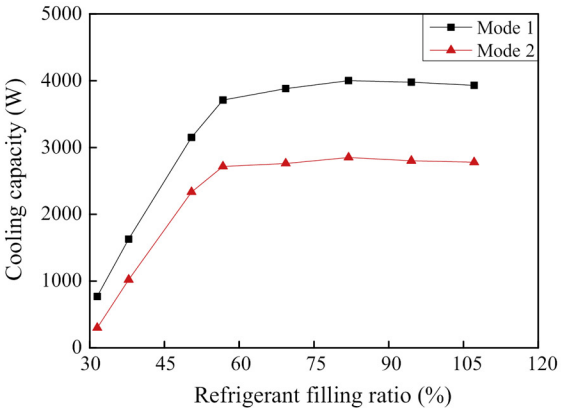

Figure 6. The cooling capacity under different refrigerant charge for different air flow rate.

superheating at the evaporator exit decreased (as shown in Figure 5). The operating temperatures and pressures of the MCSHP decreased with decreasing of the outdoor air temperature. Therefore, the superheating of the evaporator exit under Condition 4 was higher than other conditions.

In the meantime, we observed that overfilling can cause the heat transfer performance degradation of MCSHP. The cooling capacity decreased at maximum refrigerant filling ratio 120%, compared to that at the optimal refrigerant filling ratio. We inferred that, with the increase of refrigerant charge, more and more condenser surface was flooded with liquid, thereby it decreased the amount of effective condenser surface and the cooling capacity. Observed from the results, the optimal refrigerant filling ratio was 88–101% under exterior space temperature change from 8 ℃ to 23 ℃.

3.1.2. Determination of the optimal filling charge for different air volume flow rate

To determine the optimal refrigerant filling ratio for different air volume flow rates, a filter at the evaporator section was utilized. The air volume flow rate of evaporation section changed from 2980 m^3/h (Mode 1) to 1712 m^3/h (Mode 2) when a filter is added. Figure 6 shows the cooling capacity as a function of different refrigerant filling ratio at two modes. At different air volume flow rates, the cooling capacity had the same change trend: first increased rapidly, then slowed down and eventually started to decrease gradually.

With a low refrigerant filling ratio, the air volume flow rate had little effect on the cooling capacity. This is because the heat transfer resistance of the refrigerant side was dominant and the main factor of the total heat transfer coefficient. When the refrigerant filling ratio ranged from 57% to 95%, the average cooling capacity increased 40% in Mode 1 compared to Mode 2. The refrigerant in the evaporator section was mainly in two-phase state and the heat transfer coefficient of refrigerant side increased rapidly. Therefore, the total heat transfer coefficient of the evaporator was mainly affected by the air side heat transfer coefficient. According to Kim and Bullard [25] correlations, the air side heat transfer coefficient in Mode 1 and Mode 2 were 109.9 W/(m^2 K) and 82.9 W/ (m^2 K), respectively.

With an optimal refrigerant charge, the thermal resistance of the air side was calculated by Equation (6). The total thermal resistance of the evaporator section can be calculated by the measured indoor space temperature, outlet temperature of the evaporator section and cooling capacity. Table.4 shows the proportion of air side thermal resistance under Mode 1 and Mode 2 were 49.5% and 37.5%, respectively. Therefore, the air volume flow rate was the principal factor affects the cooling capacity at the optimal refrigerant filling ratio.

$$R_a = \frac{1}{\eta_0 h_a A_0} \tag{6}$$

where R_a is the thermal resistance of the air side, h_a is the air side heat transfer coefficient, A_0 is the total air side surface area, and η_0 is the surface effectiveness.

3.1.3. Effect of refrigerant filling ratio on refrigerant pressures and temperatures under standard conditions

In order to have a good understanding of the effect of refrigerant filling ratio on the thermal characteristics of MCSHP, this experiment tested refrigerant temperatures and pressures at the inlets and outlets of the evaporator section and condenser section, and the mass flow rate of condensate descending tube. Figure 7 presents the effect of refrigerant filling ratio on refrigerant pressures and mass flow rate under the standard condition. When the refrigerant filling ratio changed from 25% to 63%, the mass of liquid

Table 4. Measured operating parameters and the thermal resistance.

Type	Mode 1	Mode 2
Air flow rate (m^3/h)	2980	1712
Cooling capacity (W)	4002.11	2801.4621
Indoor space temperature (°C)	28.01	28.01
Outlet temperature of the evaporator section (°C)	23.89	22.99
Total thermal resistance (°C/W)	0.001028	0.001787
Thermal resistance of the air side (°C/W)	0.000509	0.000669
Proportion of air side thermal resistance (%)	49.5	37.5

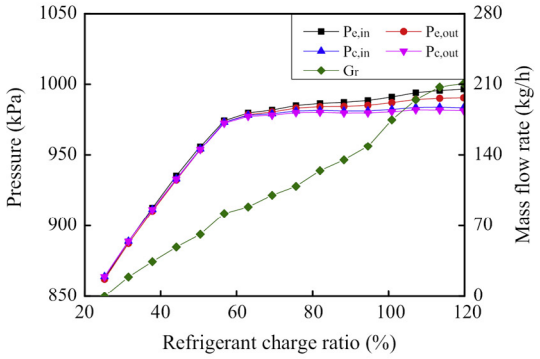

Figure 7. The refrigerant pressure and mass flow rate under different refrigerant filling ratio for standard condition.

refrigerant evaporates to gas quickly with the increase of refrigerant charge; therefore, the outlet pressure of the evaporator section increased rapidly. When the refrigerant filling ratio increased continually, the increasing rate decreased rapidly. This is because, when the refrigerant was small, the mass flow rate and the pressure drop were small as well. The increased refrigerant entered more into a vapor phase in the evaporator and led to a rapid pressure increase until the filling ratio reached the optimal region. After that, the pressure increase was constrained by the twophase mixture determined by the evaporator temperature.

Figure 8 presents the effect of refrigerant filling ratio on refrigerant temperatures, superheating and subcooling under the standard condition. The temperature difference between inlet and outlet of the evaporator and condenser section decreased with the increasing refrigerant filling ratio. At a low refrigerant filling ratio, a little refrigerant flowed into the evaporator section and transferred rapidly into saturation vapor, then superheated vapor with added heat from the air side (as shown in Figure 8, the superheating went

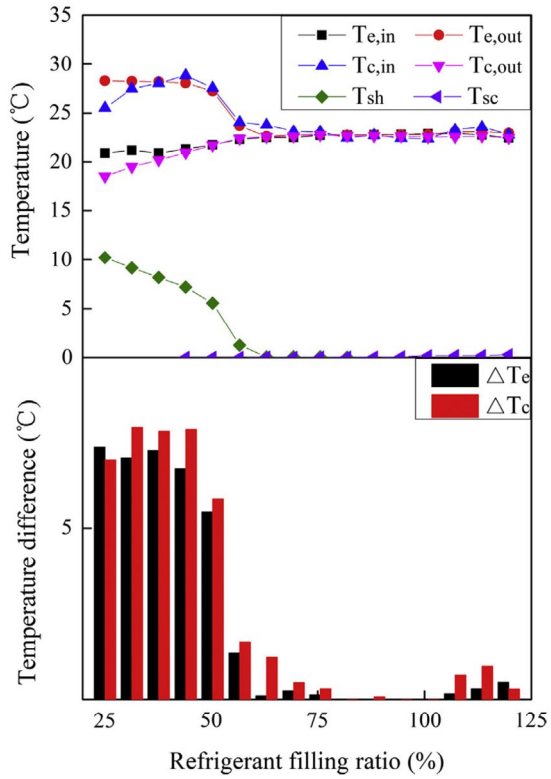

Figure 8. Refrigerant temperature, superheating and subcooling under different refrigerant filling ratios in standard condition.

up to 10 ℃ at the refrigerant filling ratio lower than 25%). The superheated vapor entered the condenser section through the vapor ascending tube and became saturated or subcooled liquid back to the evaporator section. With an increasing refrigerant filling ratio, the superheating at the exit of evaporator changed to zero gradually, and the subcooling was more than zero at the exit of the condenser section. As shown in Figure 8, the subcooling rose up to 0.17 ℃ at the refrigerant filling ratio 101%. If the refrigerant filling ratio continues to increase, it may cause excessive fluid to accumulate in the condenser section, thereby decrease the amount of effective condenser surface and the thermal performance. Figures 7 and 8 both indicated that the optimal refrigerant filling ratio was 88–101% with a low temperature difference across the evaporator and condenser section. In this range, a relatively steady pressure, low superheating of the evaporator section and low subcooling of the condenser section were observed.

3.2. Transient state response for optimal refrigerant filling ratio

In this section, we studied the transient performance of MCSHP with an optimal refrigerant filling ratio of 95%. Figure 9 presents the average of three times results about the start-up response of the MCSHP under the standard condition. It can be observed that the start-up time is about 1100 s.

In this experiment, before the fan was turned on, the system refrigerant pressure P was 1032 kPa and temperature T was 25 ℃; the refrigerant in the system was in the vapor state and the system pressures was higher than the working pressure. From 0 s to 50 s, all pressures of the refrigerant decreased rapidly because the working fan helped to condense the refrigerant vapor into liquid in the condenser section and thus reduced all pressures of refrigerant. From 50 s to 1100 s, all pressures of the refrigerant reached peaks and then decreased to relatively steady values. In this period, the refrigerant in the condenser started to condense and flowed into the evaporator section through the descending tube. The liquid refrigerant evaporated to vapor when it flowed through the evaporator section. Since the vapor mass flow rate leaving the evaporator section is probably smaller than the liquid mass flow rate entering the evaporator section, all pressures of refrigerant reached to the highest value. As time went by, the vapor mass flow rate equaled to the liquid mass flow rate, all pressures of refrigerant decreased to the relatively steady values.

3.3. Steady state response under different outdoor air temperature

At the optimal refrigerant filling ratio 95%, Figure 10 presents the cooling capacity and EER under different temperature differences between indoor and outdoor air temperatures. The outdoor

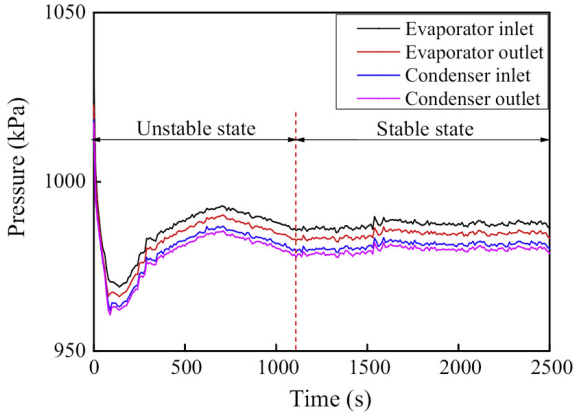

Figure 9. Startup of the MCSHP under standard condition.

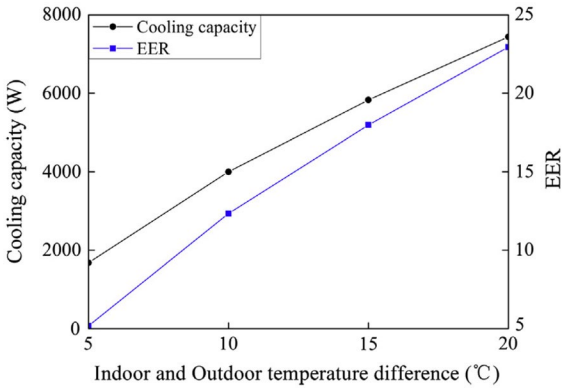

Figure 10. Cooling capacity and EER under different between indoor and outdoor temperature difference.

air temperature was varied from 8 ℃ to 23℃, while the indoor air temperature was maintained at 28 ℃. As shown in Figure 10, with the increase of temperature difference between indoor and outdoor, cooling capacity and EER increased gradually, while the increasing rate decreased slightly. The cooling capacity and EER was increased by 138% with the temperature difference between indoor and the outdoor increased from 5 ℃ to 10 ℃. Another 86% increase was achieved when the temperature difference increased from 10 ℃ to 20 ℃, which fully showed the MCSHP has a wide prospect of saving energy. With the temperature difference between indoor and outdoor increasing gradually, the working pressures and temperatures of the system decreased. It caused the temperature difference between the working fluid and indoor air as well as the cooling capacity and EER to increase. For example, when the temperature difference was 10 ℃, the EER was 12.33, distinctly higher than other cooling device for TSs.

4. Conclusions

In this paper, a micro channel heat pipe system was proposed to reduce the telecommunication station (TSs) cooling energy consumption. Various tests were carried out to determine the thermal characteristics of the MCSHP under various refrigerant filling ratios. These experiment results can be used to determine the optimal refrigerant filling ratio and optimize the system design and control. The following conclusions were drawn:

(1) The optimal refrigerant filling ratio was 88–101% under different exterior conditions and air volume flow rates. With a filling ratio in this range, the maximum cooling capacity, minimum outlet air temperature and minimum superheating of the evaporator section were achieved.
(2) For the standard condition, the MCSHP obtained a low temperature difference between the inlet and outlet of the evaporator and condenser section, relative steady pressure, low superheating at the exit of evaporator section and low subcooling at the condenser section exit under an optimal refrigerant filling ratio. Measurements on these variables could be used to detect whether the MCSHP on the optimal working state.
(3) The transient results showed about 1100 s is needed for the system. The pressures sharply decreased then increased after fans were turned on. Then, refrigerant pressures of inlet and outlet evaporator and condenser section were under steady state.
(4) The cooling capacity and EER were increased with decreasing of the air temperature of exterior space. When the temperature difference between indoor and the outdoor increased from 5 ℃ to 10℃, the cooling capacity and EER were increased by 138%. Another 86% increase was achieved when the temperature difference increased from 10 ℃ to 20 ℃, which fully showed the MCSHP has a promising prospect of saving energy application.

Acknowledgments — The present study was supported by Science and Technology of Housing and Urban, Hunan (KY201115), University of Nebraska- Lincoln Faculty Start-up Fund, International Science and Technology Cooperation Program of China (2015DFA61170), Key Project of Hunan Provincial science and Technology Department (2013WK2001) and Interdisciplinary Program of Hunan University in 2014.

References

[1] Y. Chen, Y. Zhang, Q. Meng, Study of ventilation cooling technology for telecommunication base stations in Guangzhou, Energy Build. 41 (2009) 738–744.
[2] X. Sun, Q. Zhang, M.A. Medina, S. Liao, Performance of a free-air cooling system for telecommunications base stations using phase change materials (PCMs): in-situ tests, Appl. Energy 147 (2015) 325–334.
[3] K. Ebrahimi, G.F. Jones, A.S. Fleischer, A review of data center cooling technology, operating conditions and the corresponding low-grade waste heat recovery opportunities, Renew. Sustain. Energy Rev. 31 (2014) 622–638.
[4] H. Zhang, S. Shao, H. Xu, H. Zou, C. Tian, Free cooling of data centers: a review, Renew. Sustain. Energy Rev. 35 (2014) 171–182.
[5] R. Tu, X.-H. Liu, Z. Li, Y. Jiang, Energy performance analysis on telecommunication base station, Energy Build. 43 (2011) 315–325.
[6] U. Ekstedt, M. Johansson, Heat Conducting Mounting Structure, Method and Radio Base Station Housing Arrangement for Mounting Electronic Modules, Google Patents, 2009.
[7] R.M. Weber, W.G. Wyatt, Heat Removal System for Computer Rooms, Google Patents, 2011.
[8] A. Samba, H. Louahlia-Gualous, S. Le Masson, D. Nörterhäuser, Two-phase thermosyphon loop for cooling outdoor telecommunication equipments, Appl. Therm. Eng. 50 (2013) 1351–1360.
[9] F. Zhou, J. Chen, G. Ma, Z. Liu, Energy-saving analysis of telecommunication base station with thermosyphon heat exchanger, Energy Build. 66 (2013) 537–544.
[10] H. Tian, Z. He, Z. Li, A combined cooling solution for high heat density data centers using multi-stage heat pipe loops, Energy Build. 94 (2015) 177–188.
[11] J. Zhang, Y.H. Diao, Y.H. Zhao, X. Tang, W.J. Yu, S. Wang, Experimental study on the heat recovery characteristics of a new-type flat micro-heat pipe array heat exchanger using nanofluid, Energy Convers. Manage. 75 (2013) 609–616.
[12] L. Ling, Q. Zhang, Y. Yu, Y. Wu, S. Liao, Study on thermal performance of microchannel separate heat pipe for telecommunication stations: experiment and simulation, Int. J. Refrig. 59 (2015) 198–209.
[13] S.H. Noie, Heat transfer characteristics of a two-phase closed thermosyphon, Appl. Therm. Eng. 25 (2005) 495–506.
[14] D. Liu, G.-F. Tang, F.-Y. Zhao, H.-Q. Wang, Modeling and experimental investigation of looped separate heat pipe as waste heat recovery facility, Appl. Therm. Eng. 26 (2006) 2433–2441.
[15] K.M. Armijo, V.P. Carey, An analytical and experimental study of heat pipe performance with a working fluid exhibiting strong concentration Marangoni effects, Int. J. Heat Mass Transf. 64 (2013) 70–78.
[16] J.-S. Chen, J.-H. Chou, Cooling performance of flat plate heat pipes with different liquid filling ratios, Int. J. Heat Mass Transf. 77 (2014) 874–882.

[17] J. Jin, J. Chen, Z. Chen, Development and validation of a microchannel evaporator model for a CO^2 air-conditioning system, Appl. Therm. Eng. 31 (2011) 137–146.

[18] S.-M. Kim, I. Mudawar, Universal approach to predicting two-phase frictional pressure drop for mini/micro-channel saturated flow boiling, Int. J. Heat Mass Transf. 58 (2013) 718–734.

[19] D. Reay, R. McGlen, P. Kew, Heat Pipes: Theory, Design and Applications, Butterworth-Heinemann, 2013.

[20] M.G. Khan, A. Fartaj, A review on microchannel heat exchangers and potential applications, Int. J. Energy Res. 35 (2011) 553–582.

[21] C.Y. Park, P. Hrnjak, Experimental and numerical study on microchannel and round-tube condensers in a R410A residential air-conditioning system, Int. J. Refrig. 31 (2008) 822–831.

[22] R.J. Moffat, Describing the uncertainties in experimental results, Exp. Therm. Fluid Sci. 1 (1988) 3–17.

[23] YD/T. 2770-2014, Technical requirements and experimental methods of heat pipe exchanger for communication base station, 2014 (in Chinese).

[24] GB/T 17758-2010, Unitary air conditioners, 2010 (in Chinese).

[25] M.-H. Kim, C.W. Bullard, Air-side thermal hydraulic performance of multilouvered fin aluminum heat exchangers, Int. J. Refrig. 25 (2002) 390–400.